

Ab initio DFT study of hydrogen dissociation on MoS₂, NiMoS, and CoMoS: mechanism, kinetics, and vibrational frequencies

Mingyong Sun^a, Alan E. Nelson^{a,*}, John Adjaye^b

^a University of Alberta, Department of Chemical and Materials Engineering, Edmonton, AB, Canada T6G2G6

^b Syncrude Canada Ltd., Edmonton Research Centre, Edmonton, AB, Canada T6N1H4

Received 3 March 2005; revised 10 May 2005; accepted 12 May 2005

Available online 15 June 2005

Abstract

The present study provides detailed discussions about the structures, relative stabilities, and vibrational frequencies of hydrogen species on MoS₂, NiMoS, and CoMoS catalyst edge surfaces. The transition states and activation energies for molecular hydrogen dissociation and surface migration of atomic hydrogen on catalyst edge surfaces have been calculated by complete linear synchronous transit (LST) and quadratic synchronous transit (QST) search methods. It has been found that the heterolytic dissociation of molecular hydrogen at a pair of sulfur–metal sites to form an –SH group and a metal hydride is energetically preferred. The dissociation of molecular hydrogen on the Ni-promoted (10 $\bar{1}$ 0) metal edge of NiMoS requires slightly lower activation energy than that on the unpromoted (10 $\bar{1}$ 0) Mo-edge of MoS₂ (0.87 and 0.91 eV, respectively). The dissociation of molecular hydrogen on the unpromoted ($\bar{1}$ 010) S-edge requires a large activation energy (about 1.0 eV), and the addition of cobalt to the ($\bar{1}$ 010) S-edge significantly lowers the dissociation energy to approximately 0.6 eV. The atomic hydrogen species on the ($\bar{1}$ 010) S-edge and the Co-promoted ($\bar{1}$ 010) S-edge are less mobile than on the (10 $\bar{1}$ 0) Mo-edge of MoS₂ or the Ni-promoted (10 $\bar{1}$ 0) metal edge of NiMoS. The calculated vibrational frequencies of different surface hydrogen species agree well with reported experimental observations and have provided references for further spectroscopic experiments.

© 2005 Elsevier Inc. All rights reserved.

Keywords: Hydrogen dissociation; Hydrogen migration; Hydrogen; MoS₂; NiMoS; CoMoS; Density-functional theory; Activation energy; Transition state

1. Introduction

Hydrotreating processes play an essential role in producing clean transportation fuels to meet increasingly stringent environmental regulations. Molybdenum sulfides promoted by nickel (or cobalt) have been widely used as hydrotreating catalysts for the removal of sulfur, nitrogen, and other impurities from oil fractions. Many aspects of the structures and properties of the catalytically active phase have been well defined by extensive experimental and theoretical studies [1–6]. Whereas the reaction networks of hydrodesulfurization (HDS) and hydrodenitrogenation (HDN) for many model compounds have been well documented [1,2,7], the

detailed mechanisms and energetics for elementary reactions on hydrotreating catalyst surfaces are poorly understood.

Hydrotreating reactions require the activation of hydrogen on the catalyst surface and the subsequent reactions between adsorbed hydrogen species and organic molecules. Experimental studies have shown that hydrogen and hydrogen sulfide can be adsorbed and dissociated on promoted and unpromoted molybdenum sulfide catalysts ([8], and references therein). It has previously been shown that the amount of hydrogen adsorbed at temperatures below 373 K is very low and increases with temperature, indicating that the adsorption of hydrogen on MoS₂ is an activated process [9]. Furthermore, deuterium tracer studies have shown H–D isotopic exchange between H₂ and D₂ in the presence of molybdenum sulfide catalysts [10–12]. These results indicate that hydrogen dissociates and adsorbs on MoS₂ as atomic hydrogen species, which are mobile and can recombine to

* Corresponding author. Fax: +1-780-492-2881.

E-mail address: alan.nelson@ualberta.ca (A.E. Nelson).

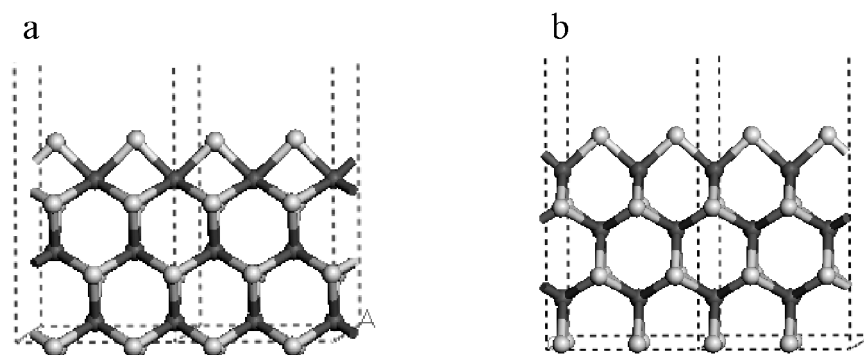


Fig. 1. Periodic models of MoS₂: (a) exposing the (10 $\bar{1}$ 0) Mo-edge on top covered by bridge sulfur atoms, and (b) exposing the ($\bar{1}$ 010) S-edge on top with 50% sulfur coverage. Dark grey, molybdenum; light grey, sulfur.

form molecular hydrogen. Possible structures of surface hydrogen species, including surface metal hydrides and –SH species, have been proposed based on experimental observations [8,9]. The relative stabilities of different hydrogen species [4,13–18] and the kinetics of hydrogen dissociation have been investigated with the use of theoretical calculations [15,19], and some of the most relevant work has been performed by Travert and co-workers [15].

The active sites of molybdenum sulfide catalysts are located at edge surfaces of the MoS₂ *hcp* layered structure [1–3]. For the (10 $\bar{1}$ 0) Mo-edge and the (1010) S-edge of unpromoted MoS₂, molybdenum atoms on the edge surfaces are covered by bridge sulfur atoms under reaction conditions [4–6,13,15,17,20]. At high H₂S concentrations, the ($\bar{1}$ 010) S-edge can be fully covered by sulfur dimers with adsorbed hydrogen [17]. For nickel-promoted MoS₂ catalysts, nickel prefers the (10 $\bar{1}$ 0) metal edge [5,6], and a fully nickel-promoted (10 $\bar{1}$ 0) metal edge (termed Ni-edge) is completely uncovered by sulfur atoms [4–6,21]. For cobalt-promoted catalysts, cobalt prefers the ($\bar{1}$ 010) S-edge, and the fully cobalt-promoted ($\bar{1}$ 010) S-edge (termed Co–S-edge) is covered by bridge sulfur atoms under reaction conditions [5,6]. Previously we studied the relative stabilities of different hydrogen species on MoS₂ and NiMoS edge surfaces [18], and the hydrogenation of pyridine and pyrrole by surface hydrogen species on Ni-promoted (10 $\bar{1}$ 0) metal edge surfaces of NiMoS [22]. In the present work, the mechanism and kinetics of hydrogen dissociation on unpromoted and promoted (10 $\bar{1}$ 0) Mo-edge and ($\bar{1}$ 010) S-edge surfaces are studied. In addition, the vibrational frequencies of hydrogen species on various edge surfaces are calculated and compared with experimental observations to validate the DFT calculations. The present results are compared with previous studies, and the implications of these results for hydrotreating reactions are discussed.

2. Methods

The calculations are based on density-functional theory (DFT) and were performed with Materials Studio DMol³ from Accelrys (version 2.2) [23]. The double-numerical

plus polarization functions (DNP) and Becke exchange [24] plus Perdew–Wang approximation [25] nonlocal functionals (GGA-PW91) are used in all calculations. The real space cutoff radius is 4.5 Å. All electron basis sets are used for light elements, such as hydrogen and sulfur. Effective core potentials [26,27] are used to treat core electrons of molybdenum and nickel, and a *k*-point of (1 × 2 × 1) was used. The convergence tolerance for energy is 2 × 10^{−5} Ha and 0.04 Ha/Å for maximum force in geometry optimization. Spin polarization was applied to all calculations for systems containing cobalt and nickel. To determine the activation energy for a specific path for the dissociation of hydrogen and diffusion of surface hydrogen species, the transition state that connects two immediate stable structures through a minimum energy path was identified by complete linear synchronous transit (LST) and quadratic synchronous transit (QST) search methods [28,29], followed by transition state confirmation through the nudged elastic band (NEB) method [30]. The parameters used in this study have been checked for convergence with an accuracy of total energy less than 0.01 eV and vibrational frequency less than 10 cm^{−1}.

The models used for the (10 $\bar{1}$ 0) metal edge (Fig. 1a) and the ($\bar{1}$ 010) S-edge (Fig. 1b) include two metal atoms along the edge surfaces (*y* direction). Along the *z* direction are three layers of MoS₂ plus terminal sulfur atoms on the edge surfaces. The MoS₂ bulk structure was optimized before cleaving to generate edge surfaces. In addition to the terminal sulfur atoms and adsorbed species, the first layer of metal atoms and a layer of sulfur atoms are free to relax during surface geometry optimization. The two bottom layers of MoS₂ are constrained to represent the bulk structure of MoS₂. The model with constrained bulk atoms and relaxed surface atoms allows accuracy similar to that of larger models with less computational time. Vacuum layers of 15 Å are applied to separate the MoS₂ slab in the *x* and *z* directions. The energy calculation results obtained with the smaller cell (2-Mo) were compared with the results obtained with larger cells including four (4-Mo) or six (6-Mo) molybdenum atoms on the edge surfaces and four layers of MoS₂ in the *z* direction. The differences in the relative energies of corresponding surface hydrogen species between 2-Mo, and 4-Mo and 6-Mo, models are within 0.1 eV, confirm-

ing that the smaller model is appropriate for this study. In addition, transition-state searches and vibrational frequency calculations used the 2-Mo model to study the mechanism and kinetics of hydrogen dissociation to obtain accurate results within a reasonable calculation time.

3. Results and discussion

3.1. On the unpromoted MoS₂ (10 $\bar{1}$ 0) Mo-edge

Table 1 summarizes the possible structures and relative energies of hydrogen species on the stable (10 $\bar{1}$ 0) Mo-edge of unpromoted MoS₂, with the clean surface and gas-phase molecular hydrogen as energetic references. The data included in brackets were obtained with the larger 6-Mo supercell, which includes six MoS₂ units along the edge surface [18]. Similar relative energies for the same structure of hydrogen species on the surface were obtained with the 2-Mo and 6-Mo models. Homolytic hydrogen dissociation to produce two –SH groups (Schemes 1e and 1f) is energetically preferred over heterolytic dissociation to yield an –SH and Mo–H pair (Schemes 1c and 1d). However, transition-state analysis indicates that there is not a direct pathway for homolytic dissociation, which connects molecular hydrogen to the two –SH groups.


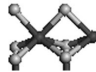
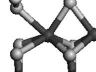


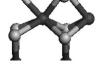
Fig. 2 shows the activation energies and the corresponding transition states of the direct formation of the H–S–H

(Path 1) and that of the Mo–H and –SH pair (Path 2) from molecular hydrogen (Scheme 1a). The heterolytic dissociation of molecular hydrogen to a pair of Mo–H and –SH requires a significantly lower activation energy (0.91 eV) compared with the formation of H–S–H (2.31 eV). Consequently, the dissociation of hydrogen would follow the lower energy path (Path 2) to generate a pair of –SH and Mo–H groups (Scheme 1c). Following the formation of an –SH and Mo–H pair, the hydrogen species on the surface can migrate across the edge surface, as shown in Fig. 3. The direct migration of hydrogen from the Mo–H to –SH (Scheme 1c to 1e) requires an activation energy of 0.39 eV. The hydrogen from the –SH group can also translate to the other side of the MoS₂ slab (Schemes 1c and 1d), a process that requires a very small activation energy of 0.12 eV. If this process occurs, the hydrogen from the Mo–H group can migrate to the terminal sulfur atom with a similar activation energy of 0.35 eV (Scheme 1d to 1f). The activation energies for all surface migration processes (0.12–0.72 eV, Fig. 3) are smaller than that for the initial dissociation process (0.91 eV, Fig. 2), which indicates the highly dynamic nature and mobility of surface hydrogen species.

In general, these results agree with those of Payen and co-workers [15,16]. They reported an activation energy of 0.97 eV for hydrogen dissociation on a S–Mo pair on the (10 $\bar{1}$ 0) Mo-edge, which is similar to the energy in the present study (0.91 eV). However, they obtained a significantly higher activation energy (0.66 eV) [16] for hydrogen transferring from one side of the MoS₂ slab to the other (Scheme 1c to 1d). In their transition state, the hydrogen is directly atop the terminal sulfur (Scheme TS2b, in Ref. [16]). The lowest activation energy pathway for hydrogen transferring from one side of the MoS₂ slab to the other side does not pass through the hydrogen-atop-sulfur transition state. Alternatively, hydrogen migrates to the other side of the MoS₂ slab by rotating around the sulfur atom, which was confirmed in the present study by the NEB method. Since this step does not involve the breaking or formation of any bonds, it should not require a high activation energy, as had been previously reported [16].

As discussed above, two –SH groups or an –SH and Mo–H pair may exist on the (10 $\bar{1}$ 0) Mo-edge plane of MoS₂ upon dissociation of molecular hydrogen. In order to support the existence of these species, the vibrational frequencies of different adsorbed hydrogen species were calculated and compared with reported spectroscopic data. The top section of Table 2 summarizes the vibrational frequencies for the –SH and Mo–H groups on the (10 $\bar{1}$ 0) Mo-edge. The –SH groups in the two structures (Schemes 1c and 1e, Table 2) have stretching frequencies around 2550 cm^{–1} and bending frequencies around 620 cm^{–1}. The Mo–H group in Scheme 1c has a stretching frequency around 1650 cm^{–1} and a bending frequency around 820 cm^{–1}. Spirko et al. reported similar calculated vibrational frequencies for the –SH group on the (10 $\bar{1}$ 0) Mo-edge, the two highest of which were 2588.6

Table 1
Relative energies and optimized surface structures of hydrogen species on the (10 $\bar{1}$ 0) Mo-edge of unpromoted MoS₂. The clean surface and gas-phase molecular hydrogen are taken as energetic references. Dark grey, molybdenum; light grey, sulfur; white, hydrogen

Scheme		ΔE (eV)/H ₂
1a		+0.00 (0.00)
1b		+0.52 (0.60)
1c		+0.08 (0.15)
1d		+0.09
1e		–0.18
1f		–0.29 (–0.20)

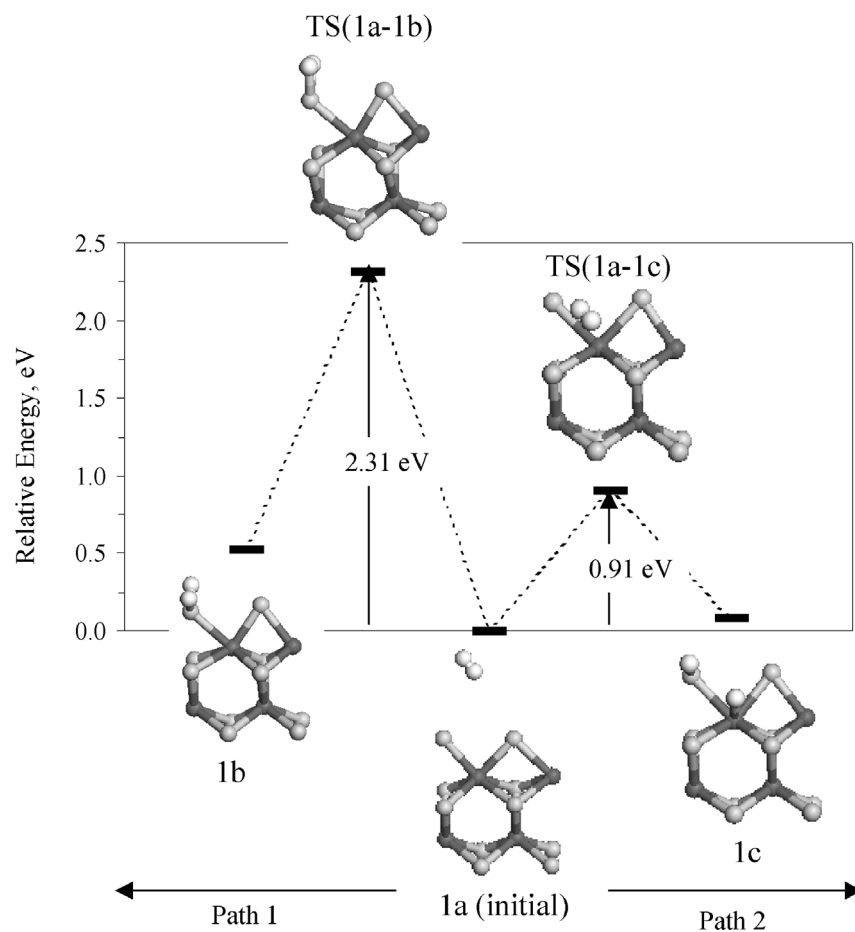


Fig. 2. Energy profile for the dissociation of molecular hydrogen on the $(10\bar{1}0)$ Mo-edge of unpromoted MoS_2 .

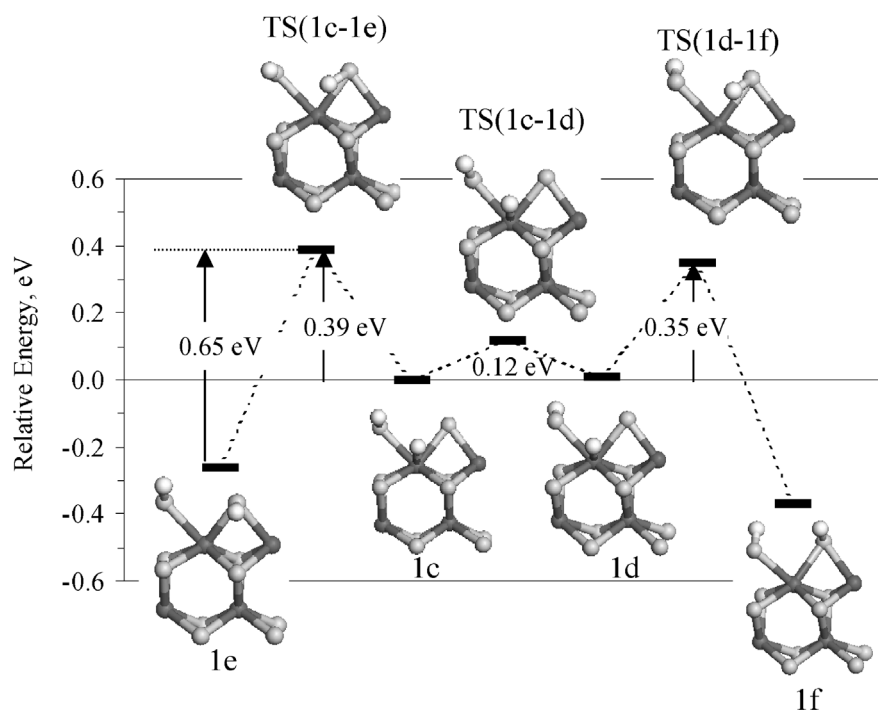
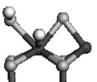




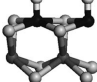

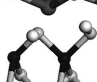


Fig. 3. Energy profile for the migration of atomic hydrogen on the $(10\bar{1}0)$ Mo-edge of unpromoted MoS_2 .

Table 2

Calculated vibrational frequencies (cm^{-1}) of atomic hydrogen species on various edge surfaces of MoS_2 , NiMoS and CoMoS catalysts. Black, nickel or cobalt; dark grey, molybdenum; light grey, sulfur; white, hydrogen

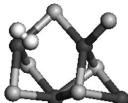
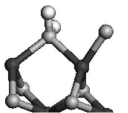
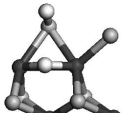
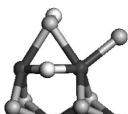
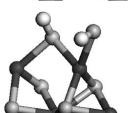

	S–H		Mo(Ni,Co)–H	
	Stretching	Bending	Stretching	Bending
Mo-edge of MoS_2				
1c 	2550	620	1650	820
1e 	2530–2550	530–630		
S-edge of MoS_2				
2c 	2550	620	1380	1150
2e 	2520–2580	540–590		
Ni-edge of NiMoS				
3c 	2580	490–730	2000	650–790
3d 			2080–2090	490–540
Co–S-edge of CoMoS				
4c 	2570	630	1930	730
4e 	2550–2590	620–760		

and 661.1 cm^{-1} ; however, they did not report the vibrational frequency for the Mo–H group on the $(10\bar{1}0)$ Mo-edge [31].

Many spectroscopic studies on the adsorption of hydrogen on MoS_2 catalysts observed bands around 2550 and 620 cm^{-1} [8,32,33], which confirms the presence of the –SH groups on the MoS_2 catalysts. However, no such spectroscopic evidence supporting the existence of Mo–H groups on the catalyst surface exists [8]. As the relative energetic data indicate, structures with two –SH groups (Schemes 1e and 1f) are about 0.3 eV more stable than the structures with one –SH group and one Mo–H group (Schemes 1c and 1d). With the use of Boltzmann population analysis [15,18], the difference in total energy (0.3 eV) can be expressed as a population ratio of Schemes 1e to 1c of approximately 200 to 1. The low concentration of Mo–H groups may explain the difficulties in recording spectroscopic frequencies corresponding to Mo–H vibrations.

Table 3

Relative energies and optimized surface structures with hydrogen species on the $(\bar{1}010)$ S-edge of unpromoted MoS_2 . The clean surface and gas-phase molecular hydrogen are taken as energetic references. Dark grey, molybdenum; light grey, sulfur; white, hydrogen

Structure		$\Delta E \text{ (eV)}/\text{H}_2$
2a 		+0.18
2b 		+0.84
2c 		+0.04
2d 		+0.16
2e 		+0.44
2f 		+0.33

3.2. On the unpromoted MoS_2 $(\bar{1}010)$ S-edge

Table 3 summarizes the possible structures and relative energies of hydrogen species on the stable $(\bar{1}010)$ S-edge of unpromoted MoS_2 , with the clean surface and gas-phase molecular hydrogen as energetic references. On the $(\bar{1}010)$ S-edge, molecular adsorption of hydrogen on either a molybdenum atom (Scheme 2a, $\Delta E = +0.18 \text{ eV}$) or a sulfur atom (Scheme 2b, $\Delta E = +0.84 \text{ eV}$), and the homolytic dissociation of molecular hydrogen to two –SH groups (Schemes 2e and 2f, $\Delta E = +0.44$ and $+0.33 \text{ eV}$, respectively) are endothermic processes. The heterolytic dissociation of molecular hydrogen to an –SH and Mo–H bridge hydride pair is athermic (Scheme 2c, $\Delta E = +0.04 \text{ eV}$). Although the –SH group prefers the *cis* configuration with the hydride (Scheme 2c vs 2d), the structure is more stable when two neighboring –SH groups are in a *trans* configuration (Scheme 2f vs 2e).

Fig. 4 shows the activation energies for the dissociation of molecular hydrogen and migration of atomic hydrogen on the $(\bar{1}010)$ S-edge of MoS_2 . The molecular adsorption of hydrogen requires a small activation energy (0.23 eV). The adsorption of molecular hydrogen activates the H–H bond, with the bond distance increased from 0.75 to 0.80 \AA . The dissociation of the adsorbed molecular hydrogen to an

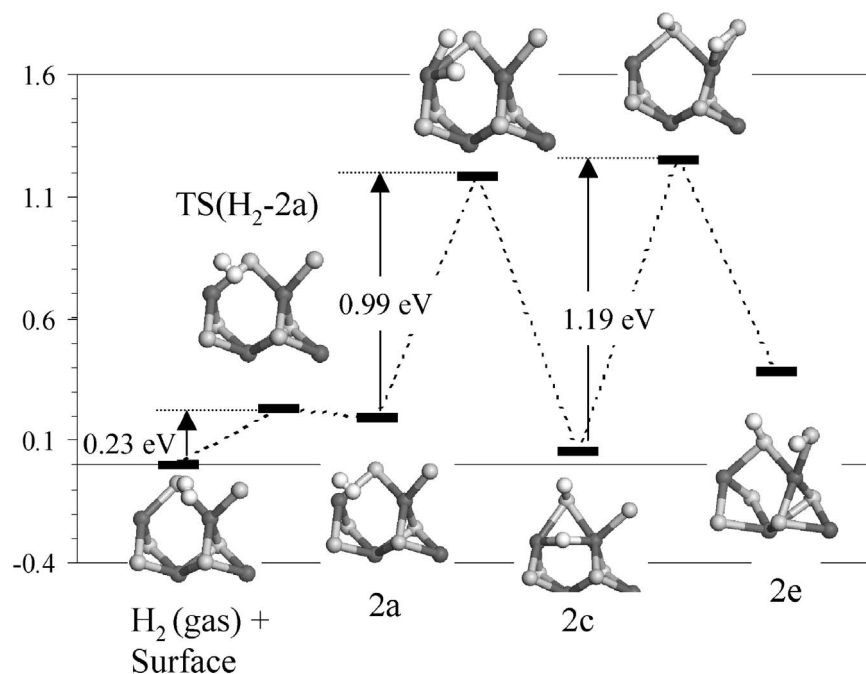


Fig. 4. Energy profile for the dissociation of molecular hydrogen and the migration of atomic hydrogen on the $(\bar{1}010)$ S-edge of unpromoted MoS_2 .

–SH group and a bridge hydride (Scheme 2a to 2c) on the $(\bar{1}010)$ S-edge of MoS_2 requires an activation energy of 0.99 eV; however, the migration of the hydride from the bridge position to a terminal sulfur atom (Scheme 2c to 2e) on the $(\bar{1}010)$ S-edge requires an even higher activation energy (1.19 eV). The hydrogen on the –SH group in Scheme 2c can translate to the other side with a small activation energy (Scheme 2c to 2d, 0.29 eV, not shown in Fig. 4). When the hydrogen on the –SH group is in the *trans* position, the migration of the hydrogen on the Mo–H still needs a very high activation energy (Schemes 2d to 2f, 1.41 eV, not shown in Fig. 4). This is considerably different from the $(10\bar{1}0)$ Mo-edge, where the dissociation of molecular hydrogen requires a higher activation energy than the surface migration of atomic hydrogen. Therefore, surface hydrogen species are less mobile on the $(\bar{1}010)$ S-edge than on the $(10\bar{1}0)$ Mo-edge, but may be mobile at high temperatures, given the moderate activation energies (less than 1.2 eV). Paul and Payen studied the dissociation of hydrogen on the unpromoted $(\bar{1}010)$ S-edge and reported a similar reaction pathway from molecular hydrogen to an –SH group and a bridge hydride (Scheme 2a to 2c), but with lower activation energies [16].

Hydrogen–deuterium exchange reactions have been used to study the kinetics of hydrogen activation on molybdenum sulfide catalyst surfaces [8,10–12]. To form HD from molecular hydrogen and deuterium, H_2 and D_2 must first dissociate, followed by the migration of surface H and D species and the formation and eventual desorption of molecular HD [10–12,15]. According to the results presented in Figs. 2–4, the H_2 – D_2 exchange reaction would be first order with respect to H_2 and D_2 when the reaction occurs on the $(10\bar{1}0)$ Mo-edge, and half-order when the reaction occurs on

the $(\bar{1}010)$ S-edge. Hensen et al. observed that the reaction on MoS_2/C was first order with respect to H_2 and D_2 [11]. Therefore, it can be concluded from the present results that the H_2 – D_2 exchange reaction occurs predominantly on the $(10\bar{1}0)$ Mo-edge, as opposed to the $(\bar{1}010)$ S-edge. This conclusion can be further supported by two explanations. First, previous work has shown that unpromoted MoS_2 clusters expose both the $(10\bar{1}0)$ Mo-edge and the $(\bar{1}010)$ S-edge and that the $(10\bar{1}0)$ Mo-edge dominates over the $(\bar{1}010)$ S-edge under typical sulfidation conditions [35,36]. Indeed, it is possible to obtain $(10\bar{1}0)$ Mo-edge exposed triangular MoS_2 clusters at very high $\text{H}_2\text{S}/\text{H}_2$ ratios [3,35,36]. Second, the reaction activation energy on the $(10\bar{1}0)$ Mo-edge is lower than that on the $(\bar{1}010)$ S-edge, especially for the migration of Mo–H. Therefore, even if the $(\bar{1}010)$ S-edge contributes to the H_2 – D_2 exchange reaction, the proportion is small compared with the $(10\bar{1}0)$ Mo-edge.

The vibrational frequencies of different adsorbed hydrogen species on the $(\bar{1}010)$ S-edge were calculated; these are summarized in Table 2. Correlating these calculated values to experimentally observed vibrational bands provides further insights. The –SH groups have similar stretching and bending frequencies around 2550 and 620 cm^{-1} , respectively, and the two highest frequencies for bridge Mo–H group are 1380 and 1150 cm^{-1} . Spirko et al. reported that the calculated vibrational frequencies were 2544.4 and 620.1 cm^{-1} for –SH, and 1222.8 and 1207.0 cm^{-1} for bridge Mo–H groups on the $(\bar{1}010)$ S-edge [31], which are similar to the frequencies in the present study. It should be noted, however, that there is only one hydrogen in their unit cell [31], which is in contrast to the model in the present study, with a pairing of –SH and bridge Mo–H groups in the unit cell.

Table 4

Relative energies and optimized surface structures with hydrogen species on the Ni-promoted (10 $\bar{1}$ 0) metal edge of NiMoS. The clean surface and gas-phase molecular hydrogen are taken as energetic references. Black, nickel; dark grey, molybdenum; light grey, sulfur; white, hydrogen

Structure	ΔE (eV)/H ₂
3a	−0.22
3b	+0.62
3c	+0.51
3d	+0.41

From the relative energetic data presented in Table 3, one can predict that the structure of Scheme 2e would exist in much lower concentrations compared with the structure of Scheme 2c on the S-edge. Furthermore, Fig. 4 shows that once the bridge Mo–H (Scheme 2c) is formed it is difficult to convert to other structures. Therefore, if molecular hydrogen is dissociated on the (10 $\bar{1}$ 0) S-edge of MoS₂ catalysts, one should be able to observe the vibrational bands for bridge

Mo–H groups at around 1150 to 1380 cm^{−1} (Table 2). Indeed, inelastic neutron scattering (INS) spectra show peaks at these regions, although they were not explicitly attributed to the Mo–H vibrations [8,34]. A high concentration of H₂S in the preparation of MoS₂ would favor the formation of the (10 $\bar{1}$ 0) Mo-edge over the (10 $\bar{1}$ 0) S-edge [35,36]. Therefore, the vibrational band around 1150 to 1380 cm^{−1} would decrease or disappear when the H₂S concentration was increased in the sulfidation mixture, or increase when the H₂S concentration was decreased.

3.3. On the Ni-promoted (10 $\bar{1}$ 0) metal edge surface

Previous studies have shown that Ni prefers to incorporate into the (10 $\bar{1}$ 0) Mo-edge of MoS₂ under normal sulfidation conditions [5,6]. Table 4 summarizes the possible structures and relative energies of hydrogen species on the Ni-promoted (10 $\bar{1}$ 0) metal edge of MoS₂, with the clean surface and gas-phase molecular hydrogen as energetic references. The adsorption of molecular hydrogen on the Ni-promoted (10 $\bar{1}$ 0) metal edge is exothermic (Scheme 3a, $\Delta E = -0.22$ eV) and nonactive (activation energy < 0.02 eV). The dissociation of adsorbed molecular hydrogen to atomic hydrogen species on the Ni-promoted (10 $\bar{1}$ 0) metal edge is endothermic (Table 3, Schemes 3b–3d).

Fig. 5 shows that the formation of two nickel hydrides from adsorbed molecular hydrogen (Scheme 3a to 3d) passes through a series of steps, and that the rate-determining step requires an activation energy of 0.87 eV (Scheme 3a to 3b). Scheme 3b presents an intermediate structure, in which one hydrogen atom bridges the nickel and the sulfur atoms. This

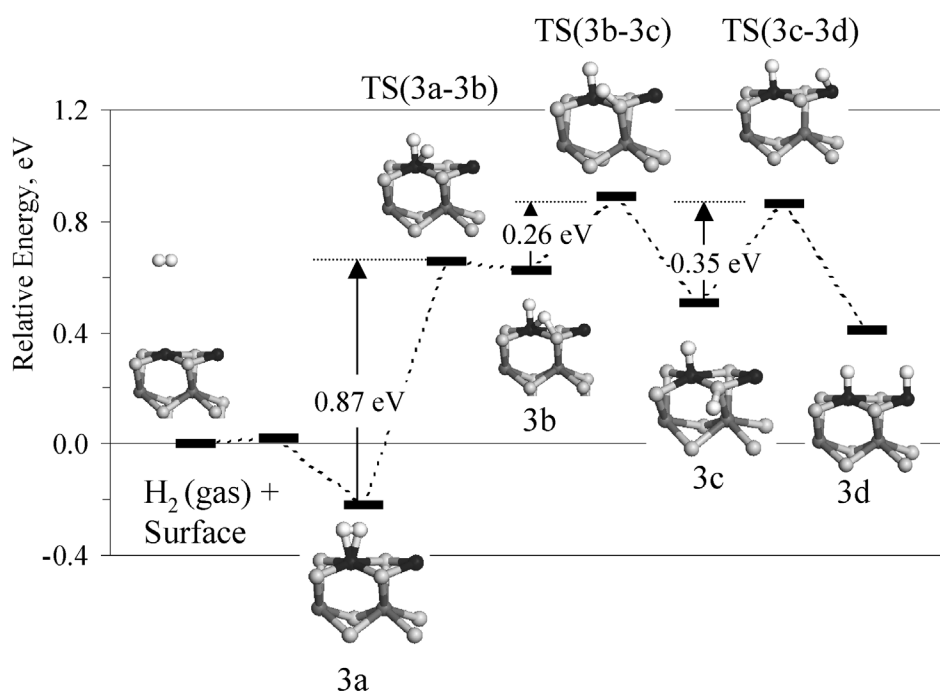


Fig. 5. Energy profile for the dissociation of molecular hydrogen and the migration of atomic hydrogen on the Ni-promoted (10 $\bar{1}$ 0) metal edge of NiMoS.

structure is not stable, and the bridge hydrogen can easily either recombine with the other hydrogen to form molecular hydrogen, or migrate over to form an –SH group on the edge of the basal plane (Scheme 3b to 3c) with a small activation energy (0.26 eV). The hydrogen on the basal plane sulfur atom can further migrate to the neighboring nickel site to form a new Ni–H group with an activation energy of 0.35 eV (Scheme 3c to 3d) on the surface. The energy barriers for surface hydrogen species to migrate on the Ni-promoted (10 $\bar{1}$ 0) metal edge surface are lower than that required for the dissociation of the adsorbed molecular hydrogen. This indicates that molecular hydrogen dissociation on the Ni-promoted (10 $\bar{1}$ 0) metal edge is rate-limiting, and, following molecular hydrogen dissociation, atomic hydrogen is very mobile.

Travert et al. studied structures of possible hydrogen species on nickel-promoted (10 $\bar{1}$ 0) metal edge surfaces with one out of three molybdenum atoms replaced by nickel [15]. On this partially Ni-promoted (10 $\bar{1}$ 0) metal edge, the surface configuration with two molybdenum atoms covered by a bridge sulfur atom is the most stable configuration compared with other edge structures. They assumed that the Mo–S(Mo,Mo) pairs were the only stable heterolytic dissociation sites for hydrogen and, therefore, that hydrogen dissociation would occur on the partly Ni-promoted (10 $\bar{1}$ 0) metal edge in the same way as on the unpromoted (10 $\bar{1}$ 0) Mo-edge [15]. They further proposed that this was the reason (or a partial reason) why nickel did not significantly promote the activity of MoS₂ for the H₂–D₂ exchange reaction [12]. The addition of nickel, however, would also reduce the number of dissociation sites by replacing molybdenum, and thus nickel should decrease the H₂–D₂ exchange reaction rate if hydrogen is only dissociated on the Mo–S(Mo,Mo) pairs. Consequently, the fully Ni-promoted (10 $\bar{1}$ 0) metal edge would have very low activity for this isotope exchange reaction because there are no such hydrogen dissociation sites. This would be the most plausible scenario for NiMoS catalysts because nickel is more stable at the (10 $\bar{1}$ 0) metal edge than other forms under sulfidation conditions [5,6]. This mechanism is still subject to debate and interpretation, however, since Thomas et al. [12] observed no significant change in the H–D exchange reaction rate with Ni-promoted MoS₂, and Lacroix et al. [10] showed that the activity of the Ni-promoted MoS₂ was twice that of unpromoted MoS₂ for H–D exchange reactions. As has been shown in Fig. 5, molecular hydrogen can be adsorbed on the nickel sites and heterolytically dissociate into a Ni–H and –SH group with a basal sulfur atom. This process requires an activation energy of 0.87 eV, only slightly lower than the activation energy required on the unpromoted (10 $\bar{1}$ 0) Mo-edge (0.91 eV), and evidence for the existence of Ni–H on the NiMoS catalysts was also reported in spectroscopic studies [8,35].

The calculated vibrational frequencies of the hydrogen species on the Ni-promoted (10 $\bar{1}$ 0) metal edge are summarized in Table 2 (Schemes 3c and 3d). The stretching frequency of the –SH group at the basal plane is similar to that

Table 5

Relative energies and optimized surface structures with hydrogen species on the Co-promoted (10 $\bar{1}$ 0) S-edge of CoMoS. The clean surface and gas-phase molecular hydrogen are taken as energetic references. Black, cobalt; dark grey, molybdenum; light grey, sulfur; white, hydrogen

Structure	ΔE (eV)/H ₂
4a	+0.51
4b	+0.37
4c	+0.01
4d	–0.01
4e	–0.81
4f	–0.87

of other –SH groups on the unpromoted edge surfaces (about 2580 cm^{–1}), but the bending frequency is slightly higher (730 cm^{–1}). The Ni–H stretching frequencies are around 2000 cm^{–1}, and the bending frequencies are around 650 and 790 cm^{–1}. The difference in relative energy between the two structures of Schemes 3c and 3d is small (0.1 eV, Table 4); thus, their concentrations should be on the same order of magnitude. In an INS study, it was reported that new peaks centered at 795 and 1895 cm^{–1} appeared after the incorporation of nickel into MoS₂, [8,35], which agree well with the calculated values corresponding to Ni–H bending and stretching vibrations on the Ni-promoted (10 $\bar{1}$ 0) metal edge of NiMoS (Table 2). Furthermore, the calculated stretching frequency for Ni–H (around 2000 cm^{–1}) corresponds very well to the INS peak reported for hydrogen adsorbed on Raney nickel [8,38].

3.4. On the Co-promoted (10 $\bar{1}$ 0) S-edge surface

Previous studies have shown that Co prefers to incorporate into the (10 $\bar{1}$ 0) S-edge of MoS₂ under normal sulfidation conditions [5,6]. Table 5 summarizes the possible structures and relative energies of hydrogen species on the stable Co-promoted (10 $\bar{1}$ 0) S-edge of MoS₂, with the clean surface and gas-phase molecular hydrogen as energetic references.

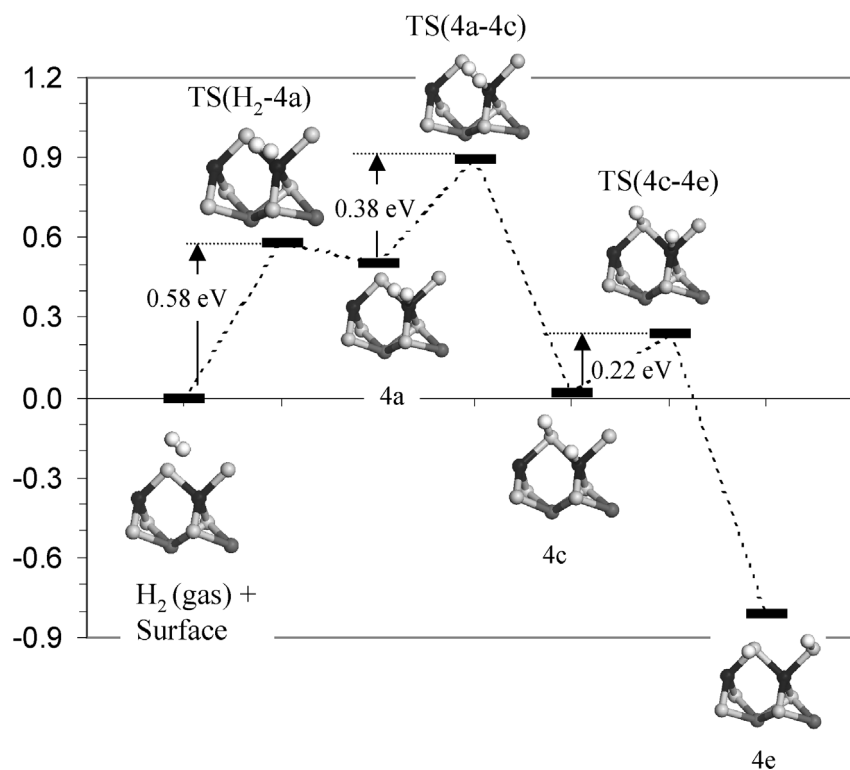


Fig. 6. Energy profile for the dissociation of molecular hydrogen and the migration of atomic hydrogen on the Co-promoted ($\bar{1}010$) S-edge of CoMoS.

The surface geometry of the Co-promoted ($\bar{1}010$) S-edge is the same as that of the unpromoted ($\bar{1}010$) S-edge, whereby terminal sulfur atoms bridge tetrahedral coordinated metal atoms. The adsorption of molecular hydrogen on an edge cobalt atom (Scheme 4a, $\Delta E = +0.51$ eV) or sulfur atom (Scheme 4b) of the promoted ($\bar{1}010$) surface is endothermic, and the formation of a pair of $-SH$ and $Co-H$ groups is athermic (Schemes 4c and 4d). The most stable hydrogen species on the Co-promoted ($\bar{1}010$) S-edge are the terminal $-SH$ groups; the formation is highly exothermic (Schemes 4e and 4f, $\Delta E = -0.81$ and -0.87 eV, respectively). This contrasts sharply with the unpromoted ($\bar{1}010$) S-edge, on which the formation of $-SH$ groups from molecular hydrogen is highly endothermic (Schemes 2e and 2f, Table 2). This is due to the weaker bonding between the sulfur atoms and the cobalt atoms on the Co-promoted ($\bar{1}010$) S-edge, which leads to a stronger interaction between the terminal sulfur and the hydrogen atom [15].

Fig. 6 presents the activation energies and corresponding transition states for the adsorption and dissociation of hydrogen on the Co-promoted ($\bar{1}010$) S-edge surface. The adsorption of molecular hydrogen on the Co-promoted ($\bar{1}010$) S-edge is an activated process, requiring an activation energy of 0.58 eV. The dissociation of adsorbed molecular hydrogen has a lower activation energy (Scheme 4a to 4c, 0.38 eV). The associatively adsorbed hydrogen is an intermediate for the formation of atomic hydrogen species on the Co-promoted ($\bar{1}010$) S-edge surface. Once atomic hydrogen species are formed, they are stable and require a much

higher activation energy to recombine to molecular hydrogen (Scheme 4c to 4a, 0.87 eV); however, the hydride from $Co-H$ can very easily migrate to the neighbor terminal sulfur atoms to form two surface $-SH$ groups on the catalyst surface (Scheme 4c to 4e, 0.22 eV). The terminal $-SH$ groups on the Co-promoted ($\bar{1}010$) S-edge are very stable, and they require an activation energy of about 1.0 eV for the hydrogen of the $-SH$ group to migrate from the terminal sulfur atom back to the neighbor cobalt site (Scheme 4e to 4c). Based on these results, the migration of atomic H (and D) would be the rate-limiting step in the H_2-D_2 exchange reactions on the Co-promoted ($\bar{1}010$) S-edge, and, thus, the rate of HD formation would be half-order with respect to H_2 and D_2 . This is exactly what was observed by Hensen et al. in their H_2-D_2 exchange experiments [11].

Travert et al. [15] also predicted that the H_2-D_2 exchange reaction on CoMoS is half-order with respect to H_2 and D_2 ; however, their model included cobalt atoms substituted on the ($10\bar{1}0$) metal edge. On the Co-promoted ($10\bar{1}0$) metal edge, the $Co-S$ bonds have some similarities with the $Co-S$ bonds on the Co-promoted ($\bar{1}010$) S-edge, and this explains why a similar conclusion about the kinetics of H_2-D_2 exchange reactions was obtained in this study. Theoretical studies have shown, however, that cobalt prefers the ($\bar{1}010$) S-edge [5,6], and cobalt was indeed observed to be located at the ($\bar{1}010$) S-edge by STM [37]. Even if cobalt could be stabilized on the ($10\bar{1}0$) metal edge, the fully Co-promoted ($10\bar{1}0$) metal edge surface with zero sulfur coverage would be more stable than the surface with bridge sulfur (Table 1,

in Ref. [15]). The bridge sulfur is not stable on the Ni-promoted or Co-promoted ($10\bar{1}0$) metal edge [4,6,15,21]. It is suggested that the Ni–S pair is more active than the Co–S pair for the H_2 – D_2 exchange reaction because the Ni–S bond is weaker than the Co–S bond [4,6,15,21]. Based on previous studies [5,6] and the results of the present work, it can be concluded that the most likely dissociation sites for CoMoS catalysts are Co–S pairs on the Co-promoted ($\bar{1}010$) S-edge with bridge sulfur, which are stable under typical sulfidation conditions. Thus, it can be concluded that it is the difference in edge preference that makes cobalt and nickel behave differently in the H_2 – D_2 exchange reaction.

The vibrational frequencies of different adsorbed hydrogen species on the Co-promoted ($\bar{1}010$) S-edge were calculated; these are summarized in Table 2. The –SH groups have slightly higher stretching frequencies on the Co-promoted ($\bar{1}010$) S-edge than on other edge surfaces (around 2580 cm^{-1}) because of a stronger interaction between the hydrogen and the sulfur in the –SH groups. This is consistent with the energetic result that the –SH groups on the Co-promoted ($\bar{1}010$) S-edge are more stable than other hydrogen species (Table 5). The Co–H stretching band is around 1930 cm^{-1} , and the bending band is around 730 cm^{-1} . These bands can distinguish the Co–H groups from the Mo–H groups on the unpromoted ($\bar{1}010$) S-edge. However, considering the large differences in relative energy (about 0.8 eV) between the structures of Schemes 4e and 4c, one can predict that the population of Co–H groups relative to the –SH groups would be below the ppm level and that the Co–H vibrational band (around 1930 cm^{-1}) could not be detected. In a Compton neutron scattering study of hydrogen adsorption on MoS_2 , CoMoS, and Co_9S_8 , Mitchell et al. [33] observed frequencies around 2500 – 2600 cm^{-1} and 650 – 670 cm^{-1} , which are associated with the S–H vibrations (Scheme 4e, Table 2), but no frequencies were observed around 1930 cm^{-1} corresponding to Co–H vibrations. The calculated energetic data and frequencies agree very well with experimental observations.

3.5. Implications for hydrotreating catalysis

In the previous sections, it has been shown that on different edge surfaces of MoS_2 -based hydrotreating catalysts, the dissociation of molecular hydrogen preferably occurs at a pair of sulfur–metal sites to form an –SH group and a metal hydride, followed by the possible migration of atomic hydrogen to a neighboring sulfur site or metal site. The differences in geometric structures and chemical properties of these sulfur–metal pairs result in the different kinetic behaviors in the catalysis of hydrogen dissociation and migration on catalyst surfaces.

On the stable unpromoted ($10\bar{1}0$) Mo-edge surface, molybdenum atoms are covered by bridge sulfur, and on the stable Ni-promoted ($10\bar{1}0$) metal edge the open nickel sites are available for different surface reactions, including hydrogen dissociation. On these ($10\bar{1}0$) metal edge surfaces,

the activation energies for hydrogen dissociation are similar (0.91 and 0.87 eV, respectively), but different hydrogen species are generated. On the ($10\bar{1}0$) Mo-edge, most of the activated hydrogen species are in the form of –SH groups, whereas on the Ni-promoted ($10\bar{1}0$) metal edge Ni–H is the major form of activated hydrogen with possibilities of –SH groups at the basal plane. Relative to molecular hydrogen and a clean catalyst surface, the hydrogen species on the Ni-promoted ($10\bar{1}0$) metal edge are less stable than on the unpromoted ($10\bar{1}0$) Mo-edge, which suggests that they are more active in reacting with organosulfur or organonitrogen species.

The ability to generate hydrogen species with higher reactivity on the surface is a key to an active hydrogenation catalyst. The Ni-promoted ($10\bar{1}0$) metal edge of NiMoS catalyst not only has such an ability; it also provides open sites for the adsorption of reacting hydrocarbons. These unique properties make NiMoS an excellent hydrogenation catalyst. In a previous study, we studied the reactions between the activated hydrogen species on the Ni-promoted ($10\bar{1}0$) metal edge and pyridine and pyrrole [22]. These surface hydrogenation reactions require only moderate activation energies (around 1.2 eV) [22], but these energies are still higher than that for hydrogen dissociation (0.87 eV). These results indicate that the dissociation of hydrogen on the Ni-promoted ($10\bar{1}0$) metal edge surface is not the rate-determining step in the hydrogenation of pyridine and pyrrole.

For CoMoS catalysts, cobalt replaces the molybdenum atoms on the ($\bar{1}010$) S-edge. Compared with the unpromoted ($\bar{1}010$) S-edge, the addition of cobalt significantly lowers the dissociation energy (to about 0.6 eV). However, the dissociated atomic hydrogen species on the ($\bar{1}010$) S-edge are much less mobile than that on the Ni-promoted ($10\bar{1}0$) metal edge because of the high stability of the Co–SH groups. The high stability and low mobility of the hydrogen species can be translated into low reactivity in subsequent surface hydrogenation reactions. This can partly explain why CoMoS is less active for hydrogenation reactions. CoMoS has a superior activity in HDS reactions and consumes less hydrogen to achieve the same level of HDS conversion as NiMoS [7]. The difference in behavior in the catalysis of hydrogen dissociation between CoMoS and NiMoS catalysts has provided some insights, but further work is required to completely reveal their different catalytic behaviors in HDS and HDN reactions.

4. Conclusions

The activation energies for hydrogen dissociation on the unpromoted ($10\bar{1}0$) Mo-edge and Ni-promoted ($10\bar{1}0$) metal edge are similar (0.91 and 0.87, respectively). The hydrogen species on the ($10\bar{1}0$) Mo-edge and the Ni-promoted ($10\bar{1}0$) metal edge are different in chemical properties, which results in different reactivities toward further surface reactions (hydrogenation). The activation energy for hydrogen dis-

sociation on the Co-promoted ($\bar{1}010$) S-edge is very low (0.58 eV), and dissociated surface hydrogen species need higher energy to migrate on the surface (around 1.0 eV). Hydrogen dissociation on unpromoted MoS₂ (mainly on the Mo-edge) and on CoMoS (on the Co-promoted S-edge) is an exothermic process, generating stable surface –SH groups. Since the Co–SH groups are more stable than the Mo–SH groups, the addition of cobalt could increase the amount of adsorbed hydrogen species on the catalyst surface. Hydrogen dissociation is an endothermic process on the Ni-promoted ($10\bar{1}0$) metal edge of NiMoS, mainly generating Ni–H on the surface. Therefore, the amount of hydrogen species on MoS₂ and CoMoS would decrease, and on NiMoS it would increase with increasing adsorption temperature. The calculated vibrational frequencies of different surface hydrogen species agree very well with experimental observations and can be used as references for further spectroscopic studies of hydrogen on molybdenum sulfide catalysts.

Acknowledgments

This work is supported by Syncrude Canada Ltd. and the Natural Sciences and Engineering Research Council (NSERC) under grant no. CRDPJ 261129.

Supplementary material

The online version of this article contains additional supplementary material.

Please visit [DOI:10.1016/j.jcat.2005.05.009](https://doi.org/10.1016/j.jcat.2005.05.009).

References

- [1] R. Prins, V.H.J. de Beer, G.A. Somorjai, *Catal. Rev. Sci. Eng.* 31 (1989) 1.
- [2] H. Topsøe, B.S. Clausen, F.E. Massoth, *Hydrotreating Catalysis*, Science and Technology, vol. 11, Springer, Berlin, 1996.
- [3] S. Helveg, J.V. Lauritsen, E. Lægsgaard, I. Stensgaard, J.K. Nørskov, B.C. Clausen, H. Topsøe, F. Besenbacher, *Phys. Rev. Lett.* 84 (2000) 951.
- [4] L.S. Byskov, J.K. Nørskov, B.S. Clausen, H. Topsøe, *J. Catal.* 187 (1999) 109.
- [5] H. Schweiger, P. Raybaud, H. Toulhoat, *J. Catal.* 212 (2002) 33.
- [6] M. Sun, A.E. Nelson, J. Adjaye, *J. Catal.* 226 (2004) 32.
- [7] T. Kabe, A. Ishihara, W. Qian, *Hydrodesulfurization and Hydrodenitrogenation*, Wiley–VCH/Kodansha, New York/Tokyo, 1999.
- [8] M. Breyse, E. Furimsky, S. Kasztelan, M. Lacroix, G. Perot, *Catal. Rev.* 44 (2002) 651.
- [9] R.B. Moyes, in: Z. Paal, P.G. Menon (Eds.), *Hydrogen Effect in Catalysis*, Dekker, New York, 1988, p. 583.
- [10] M. Lacroix, C. Dumonteil, M. Breyse, S. Kasztelan, *J. Catal.* 185 (1999) 219.
- [11] E.J.M. Hensen, G.M.H.J. Lardinois, V.H.J. de Beer, J.A.R. van Veen, R.A. van Santen, *J. Catal.* 187 (1999) 95.
- [12] C. Thomas, L. Vivier, M. Lescanne, S. Kasztelan, G. Pérot, *Catal. Lett.* 58 (1999) 33.
- [13] S. Cristol, J.F. Paul, E. Payen, D. Bougeard, S. Clémendot, F. Hutschka, *J. Phys. Chem. B* 104 (2000) 11220.
- [14] S. Cristol, J.F. Paul, E. Payen, D. Bougeard, S. Clémendot, F. Hutschka, *J. Phys. Chem. B* 106 (2002) 5659.
- [15] A. Traver, H. Nakamura, R.A. van Santen, S. Cristol, J.F. Paul, E. Payen, *J. Am. Chem. Soc.* 124 (2002) 7084.
- [16] J.F. Paul, E. Payen, *J. Phys. Chem. B* 107 (2003) 4057.
- [17] M.V. Bollinger, K.W. Jacobsen, J.K. Nørskov, *Phys. Rev. B* 67 (2003) 085410.
- [18] M. Sun, A.E. Nelson, J. Adjaye, *Catal. Today* (2005), in press.
- [19] L.S. Byskov, M. Bollinger, J.K. Nørskov, B.S. Clausen, H. Topsøe, *J. Mol. Catal. A: Chem.* 163 (2000) 117.
- [20] P. Raybaud, J. Hafner, G. Kresse, S. Kasztelan, H. Toulhoat, *J. Catal.* 189 (2000) 129.
- [21] P. Raybaud, J. Hafner, G. Kresse, S. Kasztelan, H. Toulhoat, *J. Catal.* 190 (2000) 128.
- [22] M. Sun, A.E. Nelson, J. Adjaye, *J. Catal.* 231 (2005) 223.
- [23] B. Delley, *J. Chem. Phys.* 113 (2000) 7756.
- [24] A.D.J. Becke, *Chem. Phys.* 88 (1988) 2547.
- [25] J.P. Perdew, Y. Wang, *Phys. Rev. B* 45 (1992) 13244.
- [26] M. Dolg, U. Wedig, H. Stoll, H. Preuss, *J. Chem. Phys.* 86 (1987) 866.
- [27] A. Bergner, M. Dolg, W. Kuechle, H. Stoll, H. Preuss, *Mol. Phys.* 80 (1993) 1431.
- [28] S. Bell, J.S. Crighton, *J. Chem. Phys.* 80 (1984) 2464.
- [29] S. Fischer, M. Karplus, *Chem. Phys. Lett.* 194 (1992) 252.
- [30] G. Henkelman, H. Jonsson, *J. Chem. Phys.* 113 (2000) 9978.
- [31] J.A. Spirko, M.L. Neiman, A.M. Oelker, K. Klier, *Surf. Sci.* 572 (2004) 191.
- [32] P. Ratnasamy, J.J. Fripiat, *Tans. Faraday Soc.* 66 (1970) 2897.
- [33] P.C.H. Mitchel, D.A. Green, E. Payen, A.C. Evans, *J. Chem. Soc. Faraday Trans.* 91 (1995) 4467.
- [34] P. Sundberg, R.B. Moyes, J. Tomkinson, *Bull. Soc. Chim. Belg.* 100 (1991) 967.
- [35] H. Schweiger, P. Raybaud, G. Kresse, H. Toulhoat, *J. Catal.* 207 (2002) 76.
- [36] J.V. Lauritsen, M.V. Bollinger, E. Lægsgaard, K.W. Jacobsen, J.K. Nørskov, B.C. Clausen, H. Topsøe, F. Besenbacher, *J. Catal.* 221 (2004) 510.
- [37] J.V. Lauritsen, S. Helveg, E. Lægsgaard, I. Stensgaard, B.C. Clausen, H. Topsøe, F. Besenbacher, *J. Catal.* 197 (2001) 1.
- [38] A.J. Renouprez, P. Fouilloux, G. Coudurier, D. Tocchio, R.J. Stockmeyer, *J. Chem. Soc. Faraday Trans.* 73 (1997) 1.